

1 Statistical properties of kinetic and total energy densities in 2 reverberant spaces^{a)}

3 Finn Jacobsen^{b)}

4 *Department of Electrical Engineering, Acoustic Technology, Technical University of Denmark, Building 352,*
5 *DK-2800 Kongens Lyngby, Denmark*

6 Alfonso Rodríguez Molares

7 *E.T.S.E. Telecomunicación, Universidade de Vigo, Campus Lagoas-Marcosende, E-36310 Vigo, Spain*

8 (Received 16 July 2009; revised 7 January 2010; accepted 8 January 2010)

AQ:
#1

9 Many acoustical measurements, e.g., measurement of sound power and transmission loss, rely on
10 determining the total sound energy in a reverberation room. The total energy is usually
11 approximated by measuring the mean-square pressure (i.e., the potential energy density) at a number
12 of discrete positions. The idea of measuring the total energy density instead of the potential energy
13 density on the assumption that the former quantity varies less with position than the latter goes back
14 to the 1930s. However, the phenomenon was not analyzed until the late 1970s and then only for the
15 region of high modal overlap, and this analysis has never been published. Moreover, until fairly
16 recently, measurement of the total sound energy density required an elaborate experimental
17 arrangement based on finite-difference approximations using at least four amplitude and phase
18 matched pressure microphones. With the advent of a three-dimensional particle velocity transducer,
19 it has become somewhat easier to measure total rather than only potential energy density in a sound
20 field. This paper examines the ensemble statistics of kinetic and total sound energy densities in
21 reverberant enclosures theoretically, experimentally, and numerically. © 2010 Acoustical Society of
22 America. [DOI: 10.1121/1.3304158]

23 PACS number(s): 43.55.Cs, 43.58.Bh [AJZ]

Pages: 1–XXXX

24

25 I. INTRODUCTION

26 Many acoustical measurements rely on determining the
27 sound energy in an enclosure. Examples include standardized
28 measurements of sound power and transmission loss in re-
29 verberation rooms. The total sound energy is usually esti-
30 mated by measuring the mean-square pressure (that is, the
31 potential energy density) either at a number of discrete posi-
32 tions or using a moving microphone, and much effort has
33 been spent on developing efficient averaging procedures.^{1,2}
34 The idea of measuring the total energy density rather than the
35 potential energy density on the assumption that the former
36 quantity varies less with position than the latter goes back to
37 the 1930s and has occasionally been discussed in the
38 literature.^{3,4} In the late 1970s the phenomenon was analyzed
39 using a stochastic interference model of a diffuse sound
40 field,⁵ and in the late 1980s the matter was examined experi-
41 mentally for the first time.⁶ However, until recently measure-
42 ment of the total sound energy density has required an elabo-
43 rate arrangement based on finite-difference approximations
44 using at least four pressure microphones.^{6–9} The micro-
45 phones should be amplitude and phase matched very well,

and the signal-to-noise ratio is poor because the finite-
difference signals should be time integrated,¹⁰ which is per-
haps one of the reasons why the method has not been used
much in practice. With the advent of a three-dimensional
particle velocity transducer, “Microflown,”¹¹ it has become
somewhat easier to measure kinetic and total rather than only
potential energy density in a sound field, as demonstrated a
few years ago.¹²

A recent investigation examined the ensemble statistics
of the sound power emitted by a monopole in reverberant
surroundings using Waterhouse’s random wave theory¹³ ex-
tended to the region of low modal overlap.¹⁴ Another recent
investigation used the same model to examine the ensemble
statistics of potential energy density.¹⁵ The purpose of the
present study is to examine the ensemble statistics of kinetic
and total sound energy densities in reverberant spaces theo-
retically, experimentally, and numerically.

II. THE RANDOM WAVE THEORY

A. The region of high modal overlap

The starting point of this investigation is a stochastic
pure-tone diffuse-field interference model of the sound field
in a reverberation room originally developed by
Waterhouse.¹³ This model describes the sound field as a sum
of plane waves arriving with random phase angles from ran-
dom directions,

^{a)} Portions of this work were presented in “Measurement of total sound energy in an enclosure at low frequencies,” Proceedings of Acoustics ’08, Paris, France, July 2008, pp. 3249–3254, and “The uncertainty of pure tone measurements in reverberation rooms below the Schroeder frequency,” Proceedings of Sixteenth International Congress on Sound and Vibration, Krakow, Poland, July 2009.

^{b)} Author to whom correspondence should be addressed. Electronic mail: fja@elektro.dtu.dk

$$71 \quad p(\mathbf{r}) = \lim_{N \rightarrow \infty} \frac{1}{\sqrt{N}} \sum_{n=1}^N A_n e^{j(\omega t - \mathbf{k}_n \cdot \mathbf{r})}, \quad (1)$$

72 where $p(\mathbf{r})$ is the sound pressure at position \mathbf{r} , A_n is a com-
73 plex random amplitude the phase angle of which is uni-
74 formly distributed between 0 and 2π , and \mathbf{k}_n is a random
75 wave number vector with a uniform distribution over all di-
76 rections. The corresponding particle velocity components in
77 three perpendicular directions can be written as

$$78 \quad u_x(\mathbf{r}) = \lim_{N \rightarrow \infty} \frac{1}{\sqrt{N}} \sum_{n=1}^N \frac{A_n \sin \theta_n \cos \varphi_n}{\rho c} e^{j(\omega t - \mathbf{k}_n \cdot \mathbf{r})}, \quad (2a)$$

$$79 \quad u_y(\mathbf{r}) = \lim_{N \rightarrow \infty} \frac{1}{\sqrt{N}} \sum_{n=1}^N \frac{A_n \sin \theta_n \sin \varphi_n}{\rho c} e^{j(\omega t - \mathbf{k}_n \cdot \mathbf{r})}, \quad (2b)$$

$$80 \quad u_z(\mathbf{r}) = \lim_{N \rightarrow \infty} \frac{1}{\sqrt{N}} \sum_{n=1}^N \frac{A_n \cos \theta_n}{\rho c} e^{j(\omega t - \mathbf{k}_n \cdot \mathbf{r})}, \quad (2c)$$

81 where φ_n and θ_n are the azimuth and polar angles defining
82 the wave number vector of the n th wave, and ρc is the char-
83 acteristic impedance of air.⁵ Each set of random amplitudes
84 and wave number vectors corresponds to an outcome of a
85 stochastic process, and above the Schroeder frequency there
86 is no difference between the statistics with respect to position
87 and the full ensemble statistics.^{5,14} It is easy to show that the
88 mean-square values of the pressure and each component of
89 the particle velocity can be expressed as a sum of two inde-
90 pendent squared Gaussian variables (random sums) with zero
91 mean.^{5,13} Thus, the mean-square pressure as well as the
92 mean-square value of any individual component of the par-
93 ticle velocity have a chi-square distribution with two degrees
94 of freedom (also known as the exponential distribution),^{13,16}
95 from which it follows that their relative (normalized) en-
96 semble variance is 1. (The relative variance of a stochastic
97 variable X , $\varepsilon^2\{X\}$, is the squared ratio of its standard devia-
98 tion $\sigma\{X\}$ to its expected value $E\{X\}$.) Moreover, these four
99 random variables can be shown to be statistically
100 independent.⁵ This combined with the fact that the variance
101 of a sum of independent random variables equals the sum of
102 their variances¹⁶ leads to the conclusion that the relative vari-
103 ance of the kinetic energy density is

$$104 \quad \varepsilon^2\{w_{\text{kin}}\} = \frac{\sigma^2\{w_{\text{kin},x} + w_{\text{kin},y} + w_{\text{kin},z}\}}{(E\{w_{\text{kin},x} + w_{\text{kin},y} + w_{\text{kin},z}\})^2} = \frac{3\sigma^2\{w_{\text{kin},x}\}}{9E^2\{w_{\text{kin},x}\}} = \frac{1}{3}, \quad (3)$$

105 where $w_{\text{kin},x}$, $w_{\text{kin},y}$, and $w_{\text{kin},z}$ are the kinetic densities corre-
106 sponding to the particle velocity components associated with
107 the x -, y -, and z -directions. Since the ensemble average of the
108 potential energy density must equal the ensemble average of
109 the kinetic energy density, the relative variance of the total
110 energy density becomes

$$\varepsilon^2\{w_{\text{tot}}\} = \frac{\sigma^2\{w_{\text{pot}} + w_{\text{kin}}\}}{(E\{w_{\text{pot}} + w_{\text{kin}}\})^2} = \frac{\sigma^2\{w_{\text{pot}}\} + \sigma^2\{w_{\text{kin}}\}}{4E^2\{w_{\text{pot}}\}} \quad 111$$

$$= \frac{1 + \frac{1}{3}}{4} = \frac{1}{3}. \quad (4) \quad 112$$

To summarize, in the region of high modal overlap, measur-
ing the kinetic sound energy density at one position in a
reverberation room gives the same statistical information as
measuring the potential energy density at three statistically
independent positions. No further gain is obtained by mea-
suring the total energy density. These results have been vali-
dated experimentally⁶ and, more recently, also confirmed by
a numerical implementation of the Green's function in a
room.¹²

B. The region below the Schroeder frequency

When the modal overlap cannot be assumed to be high,
the source that generates the sound field can no longer be
assumed to emit its free field sound power.¹⁴ The reason is
that the radiation impedance is affected by the random rever-
berant part of the sound field, which moreover is increased at
the source position because of coherent backscattering or
“weak Anderson localization” as predicted by Weaver and
Burkhardt.¹⁷ Besides, one can no longer expect the same
statistics with respect to position as would be found in an
ensemble of rooms.^{14,15} The resulting relative ensemble vari-
ance of the sound power emitted by a monopole has been
found, based on Eq. (1), to be

$$\varepsilon^2\{P_a\} = \frac{2}{M_s}, \quad (5) \quad 135$$

where M_s is the statistical modal overlap of the room.¹⁴ This
quantity is the product of the modal density and the statisti-
cal modal bandwidth) and can be written as

$$M_s = \frac{12\pi \ln(10) V f^2}{T_{60} c^3} = \frac{\pi A f^2}{2c^2}, \quad (6) \quad 139$$

where V is the volume of the room, T_{60} is its reverberation
time, A is the total absorption area of the room, f is the
frequency, and c is the speed of sound. A very different
modal model based on an assumption of the modal frequen-
cies being distributed according to the random matrix theory
of Gaussian orthogonal ensembles leads to almost the same
expression.¹⁸

Since the average of the squared amplitudes of the
waves that compose the sound field at any frequency and in
any room is proportional to the sound power emitted by the
source that generates the sound field, it follows that one may
expect additional ensemble variations in the kinetic and total
energy densities when the modal overlap is low. Such addi-
tional variations, reflected in an increase in the relative en-
semble variance, have recently been demonstrated for poten-
tial energy density.¹⁵ Moreover, because these additional
variations affect the pressure and the three perpendicular par-
ticle velocity components in the same way, these components

158 can no longer be assumed to be statistically independent, nor
 159 can kinetic and potential energy densities be expected to be
 160 statistically independent.

161 One can model the phenomenon by multiplying each of
 162 the original independent exponentially distributed variables
 163 in Eqs. (3) and (4) by another random variable that repre-
 164 sents the relative variations in the emitted sound power,

$$1 + W = \frac{P_a}{E\{P_{af}\}}. \quad (7)$$

166 The new variable W is normally distributed and has zero
 167 mean and a variance given by Eq. (5). It is statistically inde-
 168 pendent of the other quantities because the variations in the
 169 sound power depends only on the reverberant part of the
 170 sound pressure at the source position.¹⁴ The relative en-
 171 semble variance of the mean-square particle velocity compo-
 172 nent in an arbitrary direction now becomes

$$\begin{aligned} \varepsilon^2\{w'_{kin,x}\} &= \frac{E\{w_{kin,x}^2(1+W)^2\}}{(E\{w_{kin,x}(1+W)\})^2} - 1 \\ &= \frac{E\{w_{kin,x}^2\}E\{(1+W)^2\}}{E^2\{w_{kin,x}\}E^2\{1+W\}} - 1 \\ &= \frac{2E^2\{w_{kin,x}\}E\{(1+W)^2\}}{E^2\{w_{kin,x}\}E^2\{1+W\}} - 1 = 2(1 + E\{W^2\}) - 1 \\ &= 2\left(1 + \frac{2}{M_s}\right) - 1 = 1 + \frac{4}{M_s}, \end{aligned} \quad (8)$$

177 where $w'_{kin,x}$ is the modified kinetic energy density associated
 178 with the x -direction. [The first step in Eq. (8) follows from
 179 the general relation $\varepsilon^2\{X\} = E\{X^2\}/E^2\{X\} - 1$, the second step
 180 follows because the variables are statistically independent,
 181 and the third step follows from the fact that the relative vari-
 182 ance of $w_{kin,x}$ is unity.] This expression is identical with the
 183 relative ensemble variance of potential energy density,¹⁵

$$\varepsilon^2\{w'_{pot}\} = 1 + \frac{4}{M_s}. \quad (9)$$

185 (The modal model mentioned above leads to a very similar
 186 expression.¹⁸) In the same way, Eq. (3) becomes

$$\begin{aligned} \varepsilon^2\{w'_{kin}\} &= \frac{E\{(w_{kin,x} + w_{kin,y} + w_{kin,z})^2(1+W)^2\}}{(E\{(w_{kin,x} + w_{kin,y} + w_{kin,z})(1+W)\})^2} - 1 \\ &= \frac{E\{(w_{kin,x} + w_{kin,y} + w_{kin,z})^2\}E\{(1+W)^2\}}{(3E\{w_{kin,x}\})^2E^2\{(1+W)\}} - 1 \\ &= \frac{3E\{w_{kin,x}^2\} + 6E^2\{w_{kin,x}\}}{9E^2\{w_{kin,x}\}}(1 + E\{W^2\}) - 1 \\ &= \frac{12E^2\{w_{kin,x}\}}{9E^2\{w_{kin,x}\}}\left(1 + \frac{2}{M_s}\right) - 1 = \frac{1}{3} + \frac{8}{3M_s}, \end{aligned} \quad (10)$$

191 where w'_{kin} is the modified kinetic energy density.

192 It is apparent that the relative variance of the modified
 193 kinetic energy density is not simply one-third of the relative
 194 variance of a single component, given by Eq. (8); it is some-

what larger. The explanation is that the modified components
 are no longer independent. An alternative derivation of Eq. (10)
 could be based on the covariance between the three modified
 components of the kinetic energy density.

Note that

$$\frac{\varepsilon^2\{w'_{pot}\}}{\varepsilon^2\{w'_{kin}\}} = \frac{1 + \frac{4}{M_s}}{\frac{1}{3} + \frac{8}{3M_s}} = 3 \frac{1 + \frac{4}{M_s}}{1 + \frac{8}{M_s}} \rightarrow \begin{cases} 3 & \text{for } M_s \rightarrow \infty \\ \frac{3}{2} & \text{for } M_s \rightarrow 0, \end{cases} \quad (11)$$

which shows that the statistical advantage of determining
 kinetic rather than potential energy density is halved at low
 modal overlap because of the correlation between the three
 particle velocity components due to the varying sound
 power.

Equation (4) can be modified in the same manner,

$$\begin{aligned} \varepsilon^2\{w'_{tot}\} &= \frac{E\{(w_{kin,x} + w_{kin,y} + w_{kin,z} + w_{pot})^2(1+W)^2\}}{(E\{(w_{kin,x} + w_{kin,y} + w_{kin,z} + w_{pot})(1+W)\})^2} - 1 \\ &= \frac{3E\{w_{kin,x}^2\} + 6E^2\{w_{kin,x}\} + E\{w_{pot}^2\} + 6E\{w_{pot}\}E\{w_{kin,x}\}}{4E^2\{w_{pot}\}} \\ &\quad \times (1 + E\{W^2\}) - 1 \\ &= \frac{12E^2\{w_{kin,x}\} + 2E^2\{w_{pot}\} + 6E\{w_{pot}\}E\{w_{kin,x}\}}{4E^2\{w_{pot}\}} \\ &\quad \times \left(1 + \frac{2}{M_s}\right) - 1 \\ &= \frac{\frac{12}{9} + 2 + \frac{6}{3}}{4} \left(1 + \frac{2}{M_s}\right) - 1 = \frac{1}{3} + \frac{8}{3M_s}. \end{aligned} \quad (12)$$

Apparently, there is no statistical advantage in measuring
 total rather than kinetic energy density in the region of low
 modal overlap either.

To summarize, the stochastic model derived in the fore-
 going is based on the fundamental assumption that Eq. (1) is
 also valid in the region of low modal overlap, although there
 are additional variations in the random set of squared wave
 amplitudes, $|A_n|^2$, caused by the variations in the sound
 power emitted by the source. It is worth noting that in this
 frequency range the spatial statistics in any room depend
 strongly on whether the frequency is coinciding with a modal
 frequency or not. Equations (5), (8)–(10), and (12) express
 the relative variances associated with an ensemble of rooms
 with slightly different dimensions but the same modal over-
 lap.

III. EXPERIMENTAL RESULTS

Some experiments have been carried out in various
 rooms at the Technical University of Denmark in order to
 validate the foregoing stochastic considerations: a small
 (40 m³) lightly damped room, the same room with extra
 absorption, a large (245 m³) reverberation room, and the

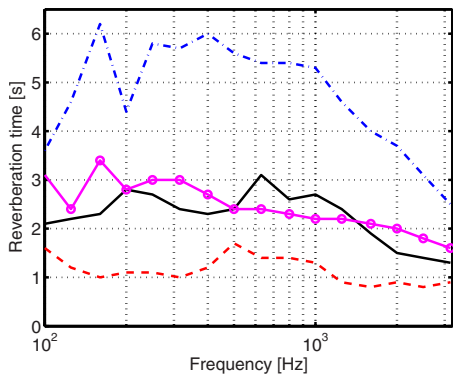


FIG. 1. (Color online) Reverberation time of the test rooms. Solid line: small lightly damped room; dashed line: small damped room; dash-dotted line: large reverberation room; line with circle markers: large damped reverberation room.

234 same large room with added absorption. The reverberation
 235 times of the four rooms are shown in Fig. 1. The correspond-
 236 ing Schroeder frequencies are 500, 330, 310, and 200 Hz,
 237 respectively. All rooms are essentially rectangular although
 238 there are large stationary diffusers in the reverberation room.
 239 The rooms were driven with a Brüel & Kjær (B&K)
 240 “OmniSource” (a loudspeaker) fitted with a B&K “Volume
 241 velocity adapter,” a device with two matched quarter-inch
 242 microphones for measuring the output volume velocity and
 243 sound power. Kinetic, potential, and total energy densities
 244 were measured at a number of positions using an “Ultimate

245 sound probe” (USP), a three-dimensional pressure-velocity
 246 probe produced by Microflow (Zevenaar, The Netherlands).
 247 The three particle velocity channels were calibrated as de-
 248 scribed in Ref. 19. The frequency responses between the vol-
 249 ume velocity of the source and the sound pressure and three
 250 perpendicular components of the particle velocity were mea-
 251 sured with a B&K “PULSE” analyzer using pseudorandom
 252 noise (6400 spectral lines) synchronized to the analysis in the
 253 frequency range up to 3.2 kHz. The experimental technique
 254 has been described in detail in Ref. 14. Obviously one cannot
 255 measure in an ensemble of rooms, so in order to approach
 256 the full variation associated with ensemble statistics, both
 257 source and receiver positions were varied. In the postpro-
 258 cessing of the results, obtained at 25 pairs of positions, ad-
 259 ditional variations over 8 Hz bands (16 adjacent frequency
 260 bins) were also taken into account to produce space-
 261 frequency variations, which can be expected to approximate
 262 the ensemble variations.¹⁴

263 Figure 2 compares the measured relative space-
 264 frequency standard deviation of a single mean-square par-
 265 ticle velocity component in an arbitrary direction with the
 266 predicted value calculated using Eq. (8). It is apparent that
 267 the results fluctuate significantly with frequency, but there is
 268 nevertheless fairly good agreement, confirming that a single
 269 mean-square particle velocity component exhibits the same
 270 statistics as the mean-square pressure. At high modal overlap
 271 the relative standard deviation approaches unity, but there is
 272 a large increase at low modal overlap. The agreement be-

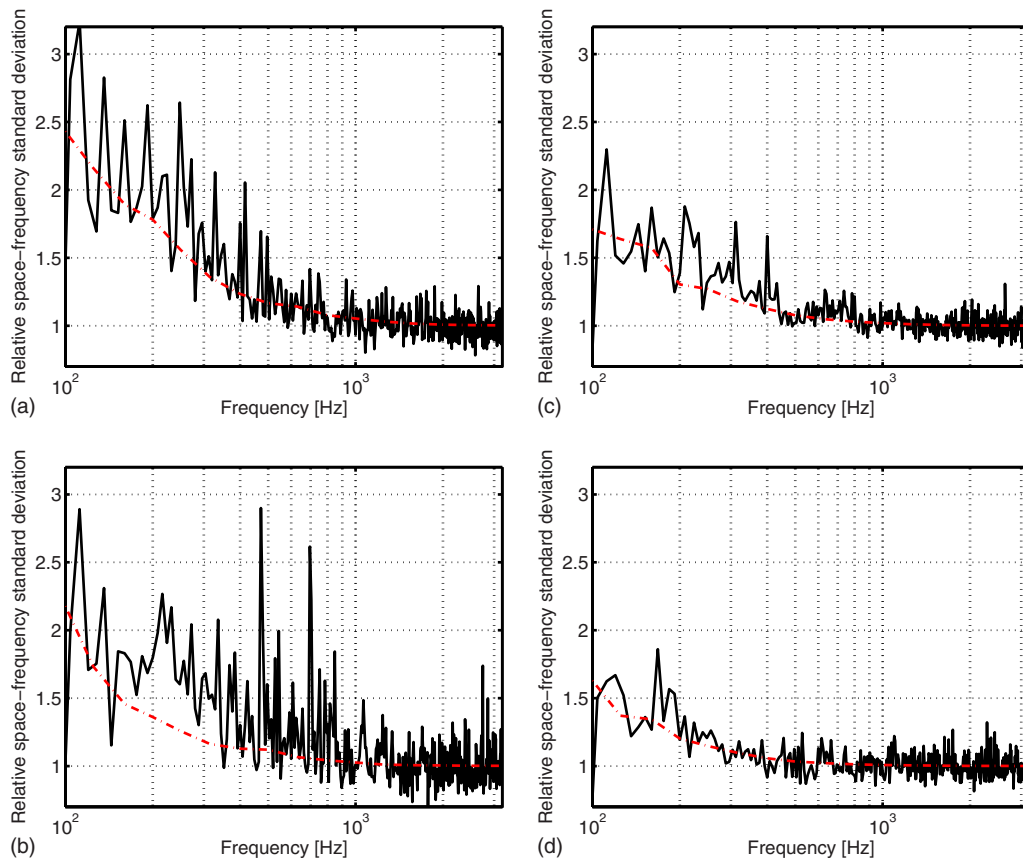


FIG. 2. (Color online) Relative space-frequency standard deviation of the mean-square value of one component of the particle velocity in (a) a small lightly damped room, (b) a small damped room, (c) a large reverberation room, and (d) a large damped reverberation room. Solid line: measured standard deviation; dash-dotted line: theory [Eq. (8)].

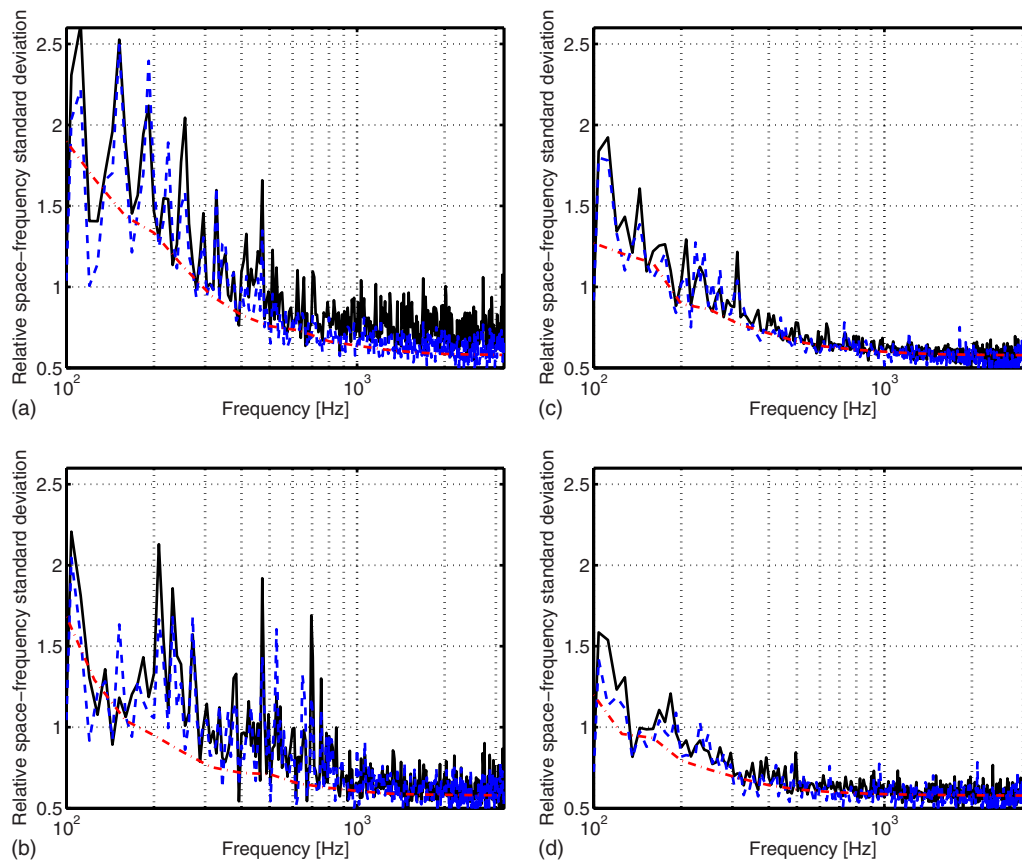


FIG. 3. (Color online) Relative space-frequency standard deviation of kinetic and total energy densities in (a) a small lightly damped room, (b) a small damped room, (c) a large reverberation room, and (d) a large damped reverberation room. Solid line: measured standard deviation of kinetic energy density; dashed line: measured standard deviation of total energy density; dash-dotted line: theory [Eqs. (10) and (12)].

273 tween measurements and predictions is better for the large
 274 room than for the small room, and for some reason Eq. (8)
 275 seems to underestimate the variations observed in the small
 276 damped room below the Schroeder frequency [Fig. 2(b)].

277 Figure 3 compares the relative space-frequency standard
 278 deviation of kinetic and total energy densities with the theory
 279 given by the identical expressions (10) and (12). The agree-
 280 ment is fairly good, confirming that the relative standard de-
 281 viation of both quantities approaches $1/\sqrt{3} \approx 0.58$ at high
 282 modal overlap and takes higher values at low modal overlap,
 283 although not as high values as the standard deviation of a
 284 single mean-square particle velocity component. In some
 285 cases the theory seems to underestimate the experimental
 286 results below the Schroeder frequency, though, but all data
 287 certainly confirm that the kinetic energy density exhibits the
 288 same statistics as the total energy density.

289 There is no obvious explanation for the tendency to un-
 290 derestimation observed in Fig. 2(b). The measurements pre-
 291 sented in Fig. 3 are more difficult since they rely on accurate
 292 calibration of the three channels of the particle velocity
 293 transducer. Inaccurate calibration of the three channels of the
 294 particle velocity transducer may have emphasized one chan-
 295 nel; this would tend to increase the experimental variance.

296 IV. NUMERICAL RESULTS

297 The full ensemble standard deviation is rather difficult to
 298 measure, but it can be estimated with a numerical model. A
 299 finite element model of 25 different rooms, constructed using

the commercial software packet ACTRAN, was used in this
 investigation. The rooms were rectangular, and their dimen-
 sions were chosen as uniformly distributed random variables
 varying between 2 and 6 m. The source positions were
 placed randomly, but they were at least 0.4 m away from any
 wall. The calculations were carried out from 200 to 300 Hz
 with a frequency step of 2 Hz. The element size was chosen
 so as to provide a low numerical pollution in the examined
 frequency range. The mean-square values of the particle ve-
 locity vector were calculated at 50 000 randomly chosen
 nodal points of the mesh. Nodes closer than 0.4 m away from
 the walls or closer than 1 m from the source were not used.
 In order to determine the relative ensemble standard devia-
 tion as a function of the modal overlap, the data were sorted
 into appropriate modal overlap intervals. A similar technique
 was used recently in Refs. 14 and 15.

Figure 4 shows the results. There is excellent agreement,
 confirming the validity of Eq. (10) and indeed of the proba-
 bilistic approach described in Sec. II. Finally Fig. 5 com-
 pares the ratio of the relative variance of potential energy
 density to the relative variance of kinetic energy density with
 the theoretical ratio given by Eq. (11). There is very good
 agreement.

V. CONCLUSION

Waterhouse's simple free-wave theory has been ex-
 tended to the region of low modal overlap and used for de-

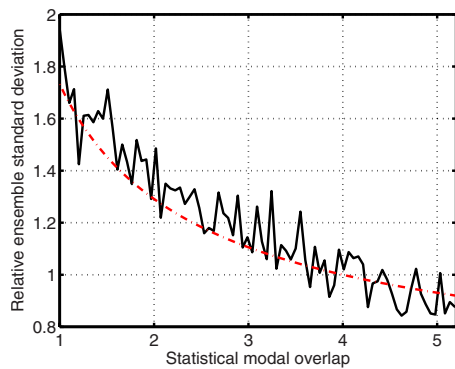


FIG. 4. (Color online) Relative ensemble standard deviation of kinetic energy density. Solid line: finite element calculations; dash-dotted line: theory [Eq. (10)].

termining the relative ensemble variance of kinetic and total energy densities in reverberation rooms, and the predictions have been confirmed by experimental and numerical results. At high modal overlap, the relative variance of both quantities approaches one-third, and it is statistically three times more efficient to measure kinetic or total energy density than to measure potential energy density. At lower modal overlap, there is an increase in the relative variance of both kinetic and total energy densities that is inversely proportional to the modal overlap, that is, proportional to the ratio of the reverberation time to the room volume and inversely proportional to the square of the frequency. In this frequency range, the statistical advantage of measuring kinetic or total energy density is reduced, and ultimately halved, because the different components of the particle velocity are no longer statistically independent.

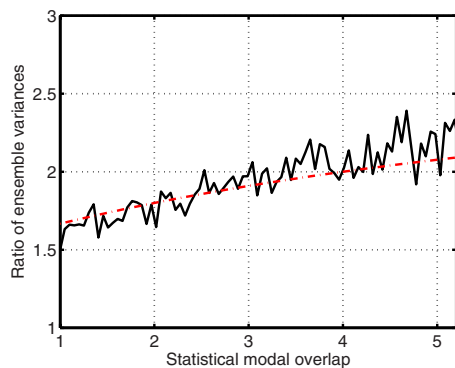


FIG. 5. (Color online) Ratio of relative variance of potential energy density to relative variance of kinetic energy density. Solid line: finite element calculations; dash-dotted line: theory [Eq. (11)].

The authors would like to thank Microflow for lending us a “USP” pressure-velocity transducer. F.J. would like to thank John Davy for suggesting approximating the variance by the space-frequency variance in the experiments.

- ¹R. V. Waterhouse and D. Lubman, “Discrete versus continuous space averaging in a reverberant sound field,” *J. Acoust. Soc. Am.* **48**, 1–5 (1970).
- ²D. Lubman, R. V. Waterhouse, and C. Chien, “Effectiveness of continuous averaging in a diffuse sound field,” *J. Acoust. Soc. Am.* **53**, 650–659 (1973).
- ³I. Wolff and F. Massa, “Direct measurement of sound energy density and sound energy flux in a complex sound field,” *J. Acoust. Soc. Am.* **3**, 317–318 (1932).
- ⁴R. K. Cook and P. A. Schade, “New method for measurement of the total energy density of sound waves,” in *Proceedings of the Inter-Noise 74*, Washington, DC (1974), pp. 101–106.
- ⁵F. Jacobsen, “The diffuse sound field,” Ph.D. thesis, Technical University of Denmark, Kongens Lyngby, Denmark (1979).
- ⁶J. A. Moryl and E. L. Hixson, “A total acoustic energy density sensor with applications to energy density measurement in a reverberation room,” in *Proceedings of the Inter-Noise 87*, Beijing, China (1987), pp. 1195–1198.
- ⁷J. W. Parkins, S. D. Sommerfeldt, and J. Tichy, “Error analysis of a practical energy density sensor,” *J. Acoust. Soc. Am.* **108**, 211–222 (2000).
- ⁸B. S. Cazzolato and J. Ghan, “Frequency domain expressions for the estimation of time-averaged acoustic energy density,” *J. Acoust. Soc. Am.* **117**, 3750–3756 (2005).
- ⁹J.-C. Pascal and J.-F. Li, “A systematic method to obtain 3D finite difference formulations for acoustic intensity and other energy quantities,” *J. Sound Vib.* **310**, 1093–1111 (2008).
- ¹⁰F. Jacobsen, “A note on finite difference estimation of acoustic particle velocity,” *J. Sound Vib.* **256**, 849–859 (2002).
- ¹¹D. R. Yntema, W. F. Druyvesteyn, and M. Elwenspoek, “A four particle velocity sensor device,” *J. Acoust. Soc. Am.* **119**, 943–951 (2006).
- ¹²D. B. Nutter, T. W. Leishman, S. D. Sommerfeldt, and J. D. Blotter, “Measurement of sound power and absorption in reverberation chambers using energy density,” *J. Acoust. Soc. Am.* **121**, 2700–2710 (2007).
- ¹³R. V. Waterhouse, “Statistical properties of reverberant sound fields,” *J. Acoust. Soc. Am.* **43**, 1436–1444 (1968).
- ¹⁴F. Jacobsen and A. Rodríguez Molaes, “Sound power emitted by a pure-tone source in a reverberation room,” *J. Acoust. Soc. Am.* **126**, 676–684 (2009).
- ¹⁵F. Jacobsen and A. Rodríguez Molaes, “The ensemble variance of pure-tone measurements in reverberation rooms,” *J. Acoust. Soc. Am.* **127**, 233–237 (2010).
- ¹⁶A. Papoulis and S. U. Pillai, *Probability, Random Variables, and Stochastic Processes*, 4th ed. (McGraw-Hill, New York, 1991).
- ¹⁷R. L. Weaver and J. Burkhardt, “Weak Anderson localization and enhanced backscatter in reverberation rooms and quantum dots,” *J. Acoust. Soc. Am.* **96**, 3186–3190 (1994).
- ¹⁸J. L. Davy, “The variance of the discrete frequency transmission function of a reverberation room,” *J. Acoust. Soc. Am.* **126**, 1199–1206 (2009).
- ¹⁹F. Jacobsen and V. Jaud, “A note on the calibration of pressure-velocity sound intensity probes,” *J. Acoust. Soc. Am.* **120**, 830–837 (2006).

NOT FOR PRINT!

FOR REVIEW BY AUTHOR

NOT FOR PRINT!

AUTHOR QUERIES — 006004JAS

#1 Au: Please check change made in title and running title.